Am J Transl Res 2018;10(11):3413-3429
www.ajtr.org /ISSN:1943-8141/AJTR0079819

Original Article

Muscular proteomic profiling of deep pressure ulcers reveals myoprotective role of JAK2 in ischemia and reperfusion injury

Zan Liu[1], Licheng Ren[1], Xu Cui[1], Le Guo[1], Bimei Jiang[2], Jie Zhou[1], Pengfei Liang[1], Jizhang Zeng[1], Zhiyou He[1], Pihong Zhang[1]

[1]*Department of Burns and Reconstructive Surgery, Xiangya Hospital, Central South University, Changsha, Hunan, P. R. China;* [2]*Department of Pathophysiology, Xiangya School of Medicine, Central South University, Changsha, Hunan, P. R. China*

Received May 17, 2018; Accepted October 18, 2018; Epub November 15, 2018; Published November 30, 2018

Abstract: Pressure ulcers (PUs) are a complex and serious clinical problem. Deep tissue injury (DTI) is either the outcome or the trigger of deep PUs. However, the cellular and molecular mechanisms that contribute to the pathogenesis of deep PUs remain unclear. In this study, the degeneration characteristics and increased autophagy and apoptosis were observed in deep PU muscle tissues. Muscular proteome of deep PU revealed that a total of 520 proteins were differentially expressed, particularly, JAK2 was down-regulated. Intriguingly, expression of JAK2 in C2C12 myoblasts exposed to oxygen-glucose deprivation and reoxygenation (OGD/R) insult was also distinctly reduced. Ex vivo, we transfected C2C12 myoblasts with lentivirus carrying the JAK2 plasmid and found that JAK2-overexpressed myoblasts exhibited a decrease in autophagy and apoptosis after OGD/R treatment, as well as less cell death. Finally, Western blot analysis determined that p-JAK2, p-AKT, p-mTOR and p-ERK1/2 levels were significantly elevated, accompanied by JAK2 overexpression but without p-STAT3, and inhibition of the AKT and ERK1/2 pathway resulted in elevated apoptosis and/or autophagy. These results demonstrated that JAK2 may play an important protective role in muscular ischemia and reperfusion injury during DTI development by inhibition of autophagy and apoptosis through the AKT and ERK1/2 pathways.

Keywords: Deep pressure ulcers, ischemia/reperfusion injury, JAK2, autophagy, apoptosis

Introduction

Pressure ulcers (PUs) are a complex and serious clinical problem, which generally occur when soft tissue is subject to mechanical deformation by long-term external load over a bony prominence. Although they are relatively uncommon in healthy subjects, they can result from excessive loading and/or sustained immobilization for those with multimorbidity and immobility [1]. PUs are a significant problem faced by global health care institutions and seriously affect patients' quality of life, morbidity and mortality, as well as healthcare costs [2, 3]. Therefore, the prevention and treatment of PUs have become increasingly important issues in today's medical field.

It is known that tissue sustaining pressure higher than that found in the blood vessels supplying the area for more than 2 h may suffer irreversible damage. Sustained deformations of the vascularized tissues (e.g., skin and muscle) resulting from prolonged compression usually leads to localized ischemia and/or subsequent unloading reperfusion, hence, a ulceration [4]. Although full-thickness PUs may be formed through progressive deterioration from the skin surface into deep tissue, the development of significant pressure-related deep tissue injury (DTI) under intact skin is another way in which PUs may aggravate [5]. A growing body of evidence suggests that ischemia and reperfusion (I/R) injury of deep tissue, especially muscle, plays a vital role in the formation and development of the overwhelming majority of PUs [5, 6]. Clinically, in most cases, the wound has been in the severe late stage by the time that the ulcer surface layer becomes visible in PUs, which makes prognosis problematic and treatment

intractable. Therefore, it is of significant clinical importance to explore the onset of the cellular process and molecular mechanism of DTI in deep PUs.

Autophagic cell death and apoptosis are two categories subdividing cell death [7]. Autophagy, also known as type II cell death, is an important natural-regulated mechanism that disassemble unnecessary or dysfunctional components in cells, being conducive to maintaining intracellular homeostasis. Studies suggested that autophagy is essential to maintain muscle mass, and proper autophagic flux is vital for both functional skeletal muscle and muscle metabolism [8]. Masiero et al. demonstrated that inhibition of autophagy resulted in considerable muscle atrophy, decreased force production and apoptosis [9]. Even though autophagy is required for cellular survival, excessive autophagy can lead to type II programmed cell death and contribute to muscle loss in different catabolic conditions [10, 11]. Apoptosis is the best-described form of programmed cell death, which plays an essential role in maintaining the fundamental homeostatic balance of cell survival and dismissal. Additionally, it is an essential component of most human diseases and, in many cases, the underlying cause of pathology. An increasing number of studies also implicate apoptosis in the catabolic and pathologic processes of skeletal muscle after major trauma or with denervation, ageing and ischemia [12-15]. Of note, autophagy and apoptosis are executed by specific proteins, and there are intricate interactions between their signaling pathways, as they share several genes/proteins that are critical for their respective execution. Moreover, numerous death stimuli may trigger either pathway, sometimes resulting in combined autophagy and apoptosis and, in other instances, switching between the two responses in a mutually exclusive manner [16]. And animal experiment revealed that both apoptotic and autophagic cell death signaling contributed to the molecular mechanism in the development of DTI [17].

Proteomics is a well-established approach to detect simultaneous protein expression with high information content in biological samples. Therefore, exploring the proteome of clinical tissue samples is an efficient, straightforward strategy for identifying key molecules and pathways associated with human diseases. Hence, we utilized quantitative, unbiased liquid chromatography-tandem mass spectrometry (LC-MS/MS) to quantify the proteome of muscle tissues in deep PU and found that JAK2 was down-regulated in PU muscle. JAK2, a member of the Janus kinase family of non-receptor cytosolic tyrosine kinases, transduces signals from ligands and activates downstream signaling pathways, especially JAK2/STAT3 [18]. Studies suggested that JAK2 plays an important role in I/R injury of several organs, such as heart, brain and kidney [19-21]. Here, we intended to explore whether JAK2 influences autophagy and apoptosis in C2C12 myoblasts exposed to I/R injury and exerts myoprotection through the AKT and ERK1/2 pathway, which may be proposed as a novel molecular target for prevention and therapy of deep PUs.

Materials and methods

Samples collection and preservation

PU muscle tissue samples were obtained from surgical specimens of patients with deep PU at Xiangya Hospital Central South University, the control group is normal muscle tissues from patients undergoing amputation or flaps operation. Clinical information of PU patients is presented in Supplementary Table 1. All samples used in this study were not identified as necrotic tissues by HE staining after operation. Informed consent was obtained from all patients before collection of tissue samples, the study was conducted in accordance with the Declaration of Helsinki and approved by the Ethics Committee of Xiangya Hospital Central South University. The samples were collected from January 2016 to December 2017, stored immediately into the liquid nitrogen after excision.

Cell culture and generation of stable cell lines

Mouse C2C12 myoblast cells (#91569) were kindly provided by Stem Cell Bank, Chinese Academy of Sciences. Cells were cultured in high glucose Dulbecco's Modified Eagle Medium (DMEM, Biological Industries, Beit HaEmek, Israel) supplemented with 10% fetal bovine serum (FBS, Biological Industries, Beit HaEmek, Israel), 100 U/mL penicillin, and 100 μg/mL streptomycin (Biological Industries, Beit HaEmek, Israel) at 37°C in a humidified incubator in mixture of 5% CO_2/95% air.

The cell transfection experiment was performed as previously described [22]. Briefly, lentiviral particles for JAK2 (LPP-Mm23982-Lv201) and the negative control (LPP-NEG-Lv201) were designed and synthesized by GeneCopoeia Inc. (Rockville, MD, USA). C2C12 cells stably overexpressing JAK2 or NEG-control were generated by infecting C2C12 cells with lentivirus carrying the EGFP-tagged JAK2 plasmid (JAK2-OE) or a negative control plasmid (NEG) at an optimal multiplicity of infection (MOI) of 100, followed by selection with puromycin (2.5 μg/mL, Sigma Aldrich, St. Louis, MO, USA).

HE staining and TUNEL staining

The muscle samples were fixed in 4% paraformaldehyde for 24 h and then dehydrated, embedded in paraffin, sliced into 5 mm thick sections according to routine procedures. The sections were then deparaffinized and hydrated with xylene and gradient ethanol respectively, followed by HE staining under classical protocol. To detect apoptotic DNA fragmentation, terminal deoxynucleotidyl transferase-mediated dUDP Nick-End Labelling (TUNEL, Roche, Indianapolis, IN, USA) staining was performed according to the manufacturer's protocol. The muscle tissue sections or fixed C2C12 cell slides were incubated with TUNEL reaction mixture in a humidified chamber at 37°C for 1 h. Then 4',6-diamidino-2-phenylindole (DAPI) was mounted to visualize nuclei. The sections and slides were scanned by Pannoramic 250 Digital Slide Scanner (3DHISTECH Ltd., Budapest, Hungary). Images were photographed and analyzed using CaseViewer 2.1 (3DHISTECH Ltd., Budapest, Hungary), the percentage of TUNEL-positive nuclei/total number of nuclei was calculated as the index of apoptosis.

Confocal immunofluorescence

C2C12 myoblast cells on glass coverslips were fixed with 4% paraformaldehyde in PBS for 15 min, permeabilized with 0.5% Triton X for 15 min, blocked with 5% donkey serum for 1 h at 37°C, then incubated overnight at 4°C with monoclonal anti-LC3 antibody (1:200, Cell Signaling Technology, Beverly, MA, USA). After washing with PBS, Alexa Fluor® 594 AffiniPure Donkey Anti-Rabbit IgG (1:400; Jackson Immuno Research, West Grove, PA, USA) was applied for 2 h at room temperature. DAPI was used to visualize nuclei according to the manufacturer's instructions. Images were obtained using a Leica TCS SP8 confocal laser scanning microscope (Leica, Mannheim, Germany). The autophagic activity, shown as LC3 puncta per cell, was evaluated using Image-Pro Plus software (Media Cybernetics, Silver Spring, MD, USA).

Transmission electron microscopy

A muscle sample with dimensions of 1 mm × 1 mm × 3 mm was removed, fixed immediately in 2.5% glutaraldehyde with phosphate buffer for 2 h, rinsed with phosphoric acid solution and fixed in 1% osmium tetroxide for 2 h, dehydrated, embedded and sliced. The blocks were cut carefully into ultrathin (50-nm) sections, counterstained with 3% uranyl acetate and lead nitrate, and then imaged with a Hitachi HT7700 Transmission Electron Microscope (Electron Microscope Research Services, Central South University, Changsha, China).

LC-MS/MS analysis

Protein from each muscle tissue sample was extracted, the protein concentration was determined with a BCA Protein Assay Kit (Thermo Scientific, Rockford, IL, USA). After being reduced, alkylated, and proteolysed with trypsin, the tryptic-digested peptides were labelled with iTRAQ according to the manufacturer's protocol, followed by fractionation with high-pH reverse-phase high-performance liquid chromatography (HPLC). Subsequently, the tryptic and labelled peptides were separated by using an EASY-nLC 1000 ultra-performance liquid chromatography (UPLC) system and then subjected to an NSI source, followed by tandem mass spectrometry (MS/MS) in a Q Exactive™ Plus (Thermo Fisher, Rockford, IL, USA) coupled online to the UPLC. The data of MS/MS were processed using the MaxQuant search engine (v.1.5.2.8) and searched against the SwissProt Human database (20130 sequences) concatenated with the reverse decoy database. A mass tolerance of 20 ppm and 0.02 Da were allowed for precursor ions in the first search and for fragment ions, respectively. FDR was adjusted to < 1%. The work was performed at PTM Biolabs Inc. (Project Number: 6622TQ, Hangzhou, China). Data are available via ProteomeXchange with identifier PXD009512.

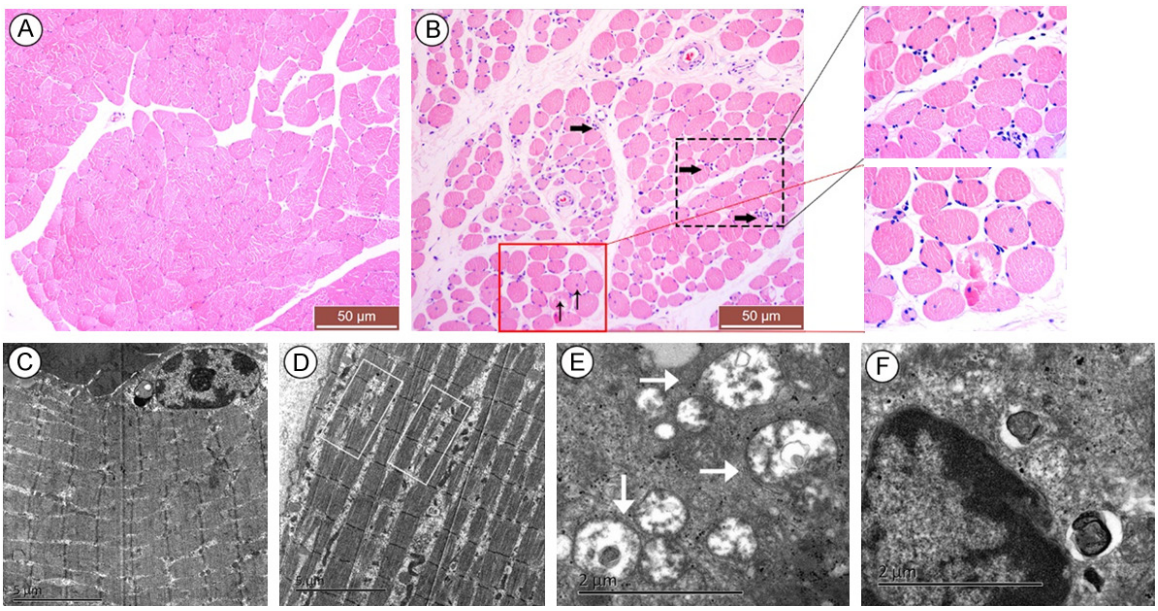

Figure 1. Histopathology of muscle tissue cells by HE staining and transmission electron microscopy. HE staining of normal muscle tissues showed an angular shape and tightly arranged myofibers with peripheral nuclei (A), while pressure ulcer (PU) muscle tissues demonstrated the morphological characteristics of degeneration, including atrophied or fractured myofibers with a round shape, increased endomysium distance between the fibers, accumulated nuclear aggregation in the interstitial space (as demonstrated by the black thick arrow) and presence of centralized myonuclei (as demonstrated by the black thin arrow); insets are higher magnification (B). However, the ultrastructure of the normal tissue indicated clear internal fine structure and orderly tight arrangement of sarcomeres (C), while PU muscle cells revealed loosely arranged, lysed and discontinued sarcomeres (as demonstrated by the white rectangle in D), swollen denatured mitochondria (as demonstrated by the white thick arrow in E), as well as chromatin margination (F). The scale was shown in corresponding picture.

Bioinformatics analysis

In this study, fold-change ≥ 2.0 with $P < 0.05$ was considered the standard of differential expression. Gene Ontology (GO) annotation of the proteome was derived from the UniProt-GOA database (http://www.ebi.ac.uk/GOA/) and used for screening of autophagy- and apoptosis-related proteins from identified proteins based on biological process and molecular function. Then, the Kyoto Encyclopedia of Genes and Genomes (KEGG) databases (http://www.genome.jp/kegg/) were applied to annotate the pathways of those proteins. Ultimately, aiming to evaluate the interactive relationships among the autophagic and apoptotic proteins, those identified proteins were inputted into the STRING database (http://string.embl.de/) to obtain the protein-protein interaction (PPI) network. A confidence score ≥ 0.7 (high confidence) was chosen as the cut-off criterion.

Western blot analysis

In brief, total protein was extracted from skeletal muscle or C2C12 cells using protein extraction reagents. The protein concentrations were determined using a BCA kit (Thermo Scientific, Rockford, IL, USA). Tissue proteins were separated by electrophoresis on TGX Stain-Free™ FastCast™ Acrylamide Kit (Bio-Rad, Hercules, CA, USA) while cell proteins on SDS-PAGE, then transferred to polyvinylidene fluoride (PVDF) membranes. After blocking with 5% bovine serum albumin, membranes were incubated with primary antibodies (shown in Supplementary Table 2) overnight at 4°C, followed by secondary antibody for 2 h. The protein bands were visualized with Chemi Doc™ Imaging System (Bio-Rad, Hercules, CA, USA). Relative expression levels were analyzed using Image J software (National Institutes of Health, Bethesda, MD, USA) and were normalized to total protein or β-actin.

Oxygen-glucose deprivation and reoxygenation (OGD/R) experiment

OGD/R experiment was applied as an in vitro model of I/R injury. The experiment was performed with minor modifications, as previously described by Hsu et al. [23]. Briefly, mouse

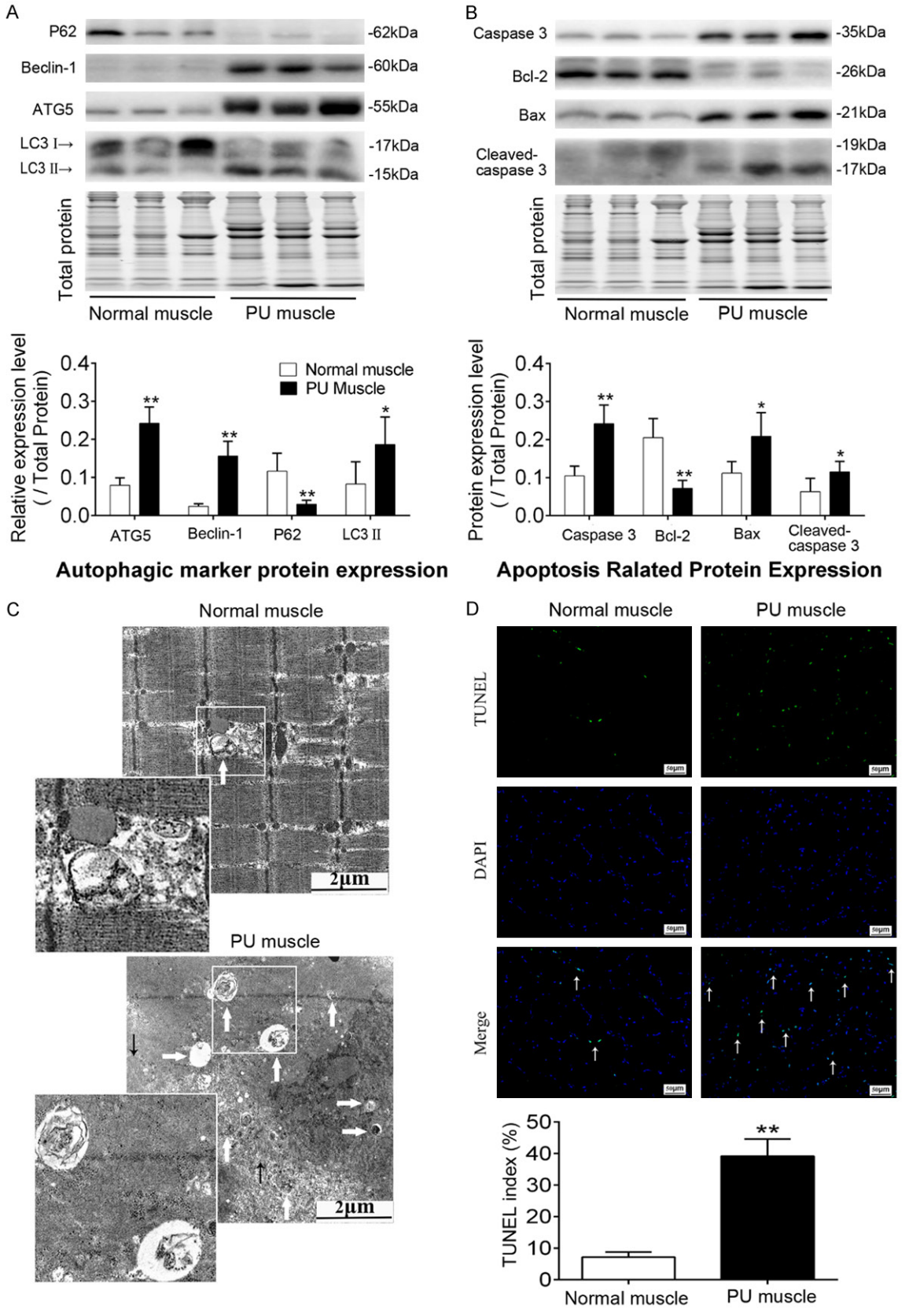

Figure 2. Elevations in autophagy and apoptosis in deep PU muscle tissue compared with normal muscle. A. Representative immunoblot images and relative quantification of P62, Beclin1, ATG5 and LC3, collectively as an index

of autophagy level. B. Representative immunoblot images and relative quantification of Bcl-2, Bax, Caspase 3 and cleaved Caspase 3, collectively as an index of apoptosis level. TGX Stain-Free™ FastCast™ Acrylamide Gel was performed to assess the total amount of protein expression, which was used for normalization. C. Transmission electron micrographs of autophagosomes in normal and PU muscle samples. Insets are higher magnification. White thick arrows and black thin arrows indicate autophagosomes and myofilament, respectively. D. Up panel: photomicrographs of TUNEL staining for normal and PU muscles, white thin arrows show TUNEL-positive nuclei; Down panel: quantitative analysis of the number of apoptotic cells, shown as TUNEL index. The scale was shown in corresponding picture, (n = 5-8; Means ± SD; *$P < 0.05$, **$P < 0.01$).

C2C12 myoblast cells were cultured in 6-well plates for 36 h at a density of 1×10^6 cells/well. To induce the OGD/R insult, the standard culture media were replaced with deoxygenated glucose-free and serum-free DMEM at pH 7.4, then the cells were transferred into a hypoxic chamber (Don Whitley Scientific DG250, Shipley, UK) containing a mixture of 5% CO_2, 10% H_2 and 85% N_2 at 37°C for 6 h. OGD was terminated by replacing the deoxygenated glucose-free and serum-free DMEM with standard medium and then returning the cells to normoxic culture conditions (37°C, 5% CO_2) for 2 h. Control cells were treated with standard media and cultured in normal conditions (37°C, 5% CO_2). At the end of the OGD/R treatment, cells were harvested immediately for TUNEL staining and Western blotting. To inhibit PI3K/AKT and ERK1/2 pathways, 10 μM LY294002 and 10 μM U0126 (Sigma-Aldrich, St Louis, MO, USA) were added to the medium 30 min before each experiment correspondingly [24, 25].

Cell viability assay

Cell survival was determined using Cell Counting Kit-8 (CCK8, 7 Sea, Shanghai China). Briefly, C2C12 cells were cultured in a 96-well plate at a density of 5×10^3 cells/well. After 24 h, the cells were exposed to OGD for 6 h and reperfusion for 2-8 h, then treated with 10 μL CCK-8 solution each well, incubated for 4h at 37°C. Absorbance at 450 nm was measured using an infinite M200 PRO microplate reader (Tecan Group Ltd., Männedorf, Switzerland). Percent viability (%) = absorbance of OGD-treated group/absorbance of control group). The experiment was repeated for 3 times.

Statistical analyses

Data were presented as the means ± standard deviation (SD). Statistical significance was determined by one-way ANOVA analysis followed by LSD for multiple comparisons and unpaired Student's t test for comparison between two groups. Statistical analyses were performed using GraphPad Prism software version 6 (GraphPad Software Inc., San Diego, CA, USA). $P < 0.05$ was considered statistically significant.

Results

Muscle tissue histopathological analysis

According to the morphology of muscle tissues by HE staining, normal muscle generally showed an angular shape, uniform peripheral nuclei, and close arrangement of myofibers (**Figure 1A**), while pathohistological characteristics, including atrophied or fractured myofibers with a rounded shape, increased endomysium distance between the fibers, accumulated nuclei aggregation in the interstitial space and centralized myo-nuclei, were demonstrated in PU muscle (**Figure 1B**). Compared with normal muscle with a clear internal fine structure and an orderly, tight arrangement of sarcomeres (**Figure 1C**), the ultra-structure of PU muscle showed loosely arranged, lysed and discontinued sarcomeres (**Figure 1D**). In addition, mitochondrial swelling and vacuolar degeneration, which are usually induced by endoplasmic reticulum stress (ERS), were obvious (**Figure 1E**). Chromatin margination, which suggests muscle cell apoptosis, was also observed (**Figure 1F**).

Autophagic and apoptotic changes in deep PU muscle tissues

Western blot analysis of autophagic and apoptotic marker proteins between PU muscle and normal muscle was performed, as along with TUNEL staining used for identifying apoptotic muscle-associated nuclei. The results showed that Beclin1 and ATG5, autophagic factors that are important for induction and formation of a pre-autophagosome structure, along with LC3II, were found to be significantly increased in PU muscle, whereas P62, a substrate drives

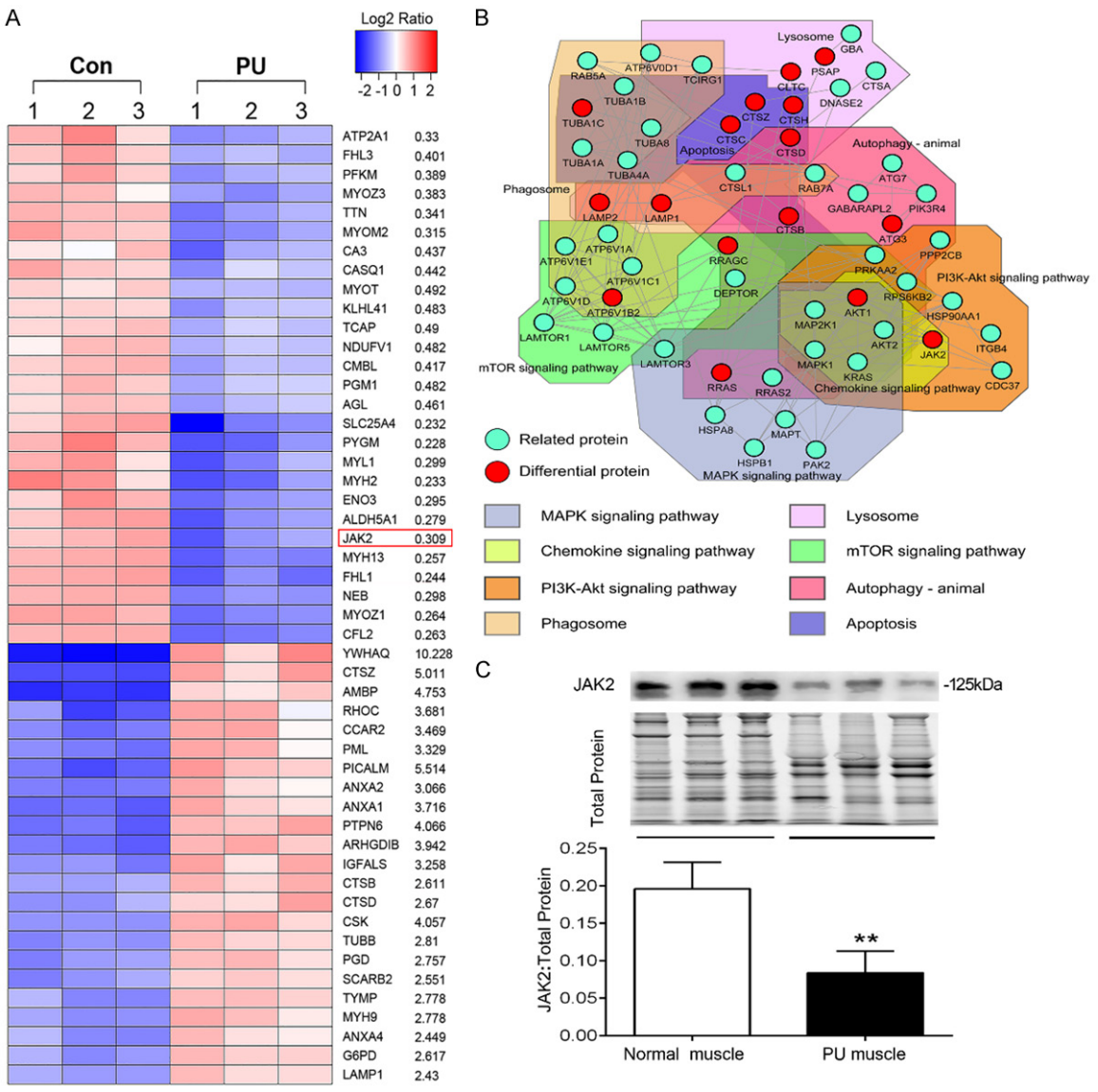

Figure 3. The protein expression profile of deep PU muscle and western blot validation. A. Heat map exhibiting a part of the significantly differentially expressed proteins in PU muscle compared with normal muscle. Peptide levels were from the proteomics analysis, $P < 0.05$ and fold change ≥ 2 were the cut-off (in order of P value). B. The protein-protein interaction network of autophagy- and apoptosis-associated proteins obtained from the STRING database with a confidence score of ≥ 0.7 containing 54 nodes and 146 edges, with pathway analysis of those proteins. C. Representative immunoblot images and relative quantification of JAK2 for PU muscles and normal muscles. TGX Stain-Free™ FastCast™ Acrylamide Gel was performed to assess the total amount of protein expression, which was used for normalization (n = 5-8; Means ± SD; $^{**}P < 0.01$).

both LC3 and ubiquitinated proteins to degradation during autophagy, was enormously decreased in PU muscle (**Figure 2A**). These results were consistent with the findings of transmission electron microscopy, in which an increase in double membrane structures containing cytoplasm or intracellular organelles (i.e., the autophagosomes) was observed in PU muscle compared with normal muscle (**Figure 2C**). Furthermore, the apoptotic factor caspase 3 and cleaved caspase 3 and the pro-apoptotic protein Bax were increased in PU muscle, while the anti-apoptotic protein Bcl-2 was decreased (**Figure 2B**). Additionally, the number of TUNEL-positive muscle cells and the index of apoptosis were significantly elevated in PU muscle tissues relative to normal muscle (**Figure 2D**). Altogether, the results above indicated that

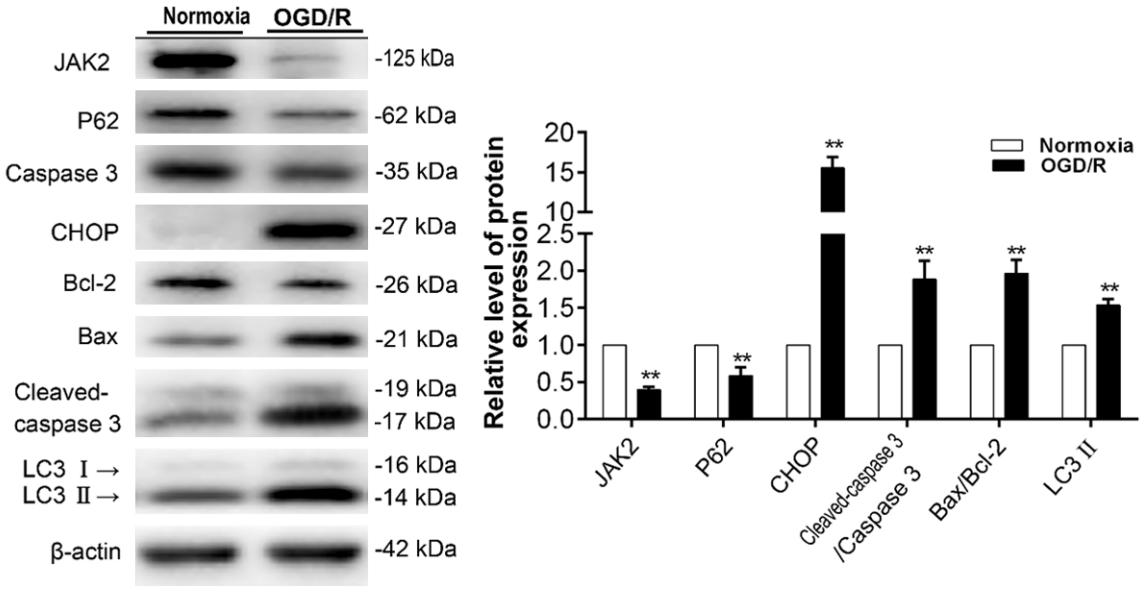

Figure 4. Autophagic and apoptotic response induced by OGD/R in mouse C2C12 myoblast cells. Representative immunoblot images and relative quantification of JAK2, P62, Caspase 3, CHOP, Bcl-2, Bax, cleaved Caspase 3, LC3 and β-actin in C2C12 myoblasts treated with normoxia (control group) and OGD/R. Quantification expressed as fold induction over control group (assumed as 1), data were determined by densitometric analysis from at least 3 independent experiments after normalization by β-actin (Means ± SD; $^{**}P < 0.01$ versus control group).

both autophagy and apoptosis were augmented in deep PU muscle.

Proteomics and bioinformatics analysis

To explore the proteome in deep PU muscle, the total proteins of deep PU muscle and normal muscle were extracted for iTRAQ LC-MS/MS analysis. Hierarchical clustering analysis was applied accordingly to all detected proteins and those differentially expressed proteins (**Figure 3A**). Among the 2558 detected proteins, 427 and 93 proteins were up-regulated and down-regulated in deep PU muscle, respectively. Considering that significant alteration of autophagy and apoptosis in deep PU muscle tissues, therefore, the autophagy- and apoptosis-associated proteins based on muscular proteomics were identified for pathway analysis, along with protein-protein interaction network construction. The result suggested that those proteins were involved in a number of pathways, such as phagosome, MAPK, and the PI3K/AKT signaling pathway. Furthermore, some proteins had more than one interaction with each other, such as JAK2, AKT, and Cathepsin B (**Figure 3B**). JAK2, the upstream kinase activating the canonical JAK2/STAT3 pathway and noncanonical MAPK and PI3K/AKT pathways, plays an important role in I/R injury of several organs and tissues. Consequently, immunoblotting confirmed that JAK2 distinctly down-regulated in deep PU muscle tissues (**Figure 3C**). Given the poor understanding of its role in development of deep PUs and its multiple interaction with other autophagy- and apoptosis-associated proteins and involvement in multiple signaling pathways (**Figure 3B**), we further explored the role of JAK2 in muscular I/R injury.

Autophagic and apoptotic response is induced by OGD/R in C2C12 myoblast cells

First, we verified whether experimentally induced oxygen-glucose deprivation and reoxygenation (OGD/R) insult occurred in C2C12 myoblast cells. The cell viability assay result showed cells treated with hypoxia 6 h and reoxygenation 2 h (H6R2) suffered the worst insult (Supplementary Figure 1). Next, the expression of autophagic and apoptotic marker proteins in myoblasts exposed to OGD/R was detected by immunoblotting. As shown in **Figure 4**, the expression of LC3II and the ratios of Bax/Bcl-2 and cleaved caspase 3/caspase 3 were increased after OGD/R insult, while intracellular p62 was depleted, suggesting that both autophagy and apoptosis were elevated during OGD/R

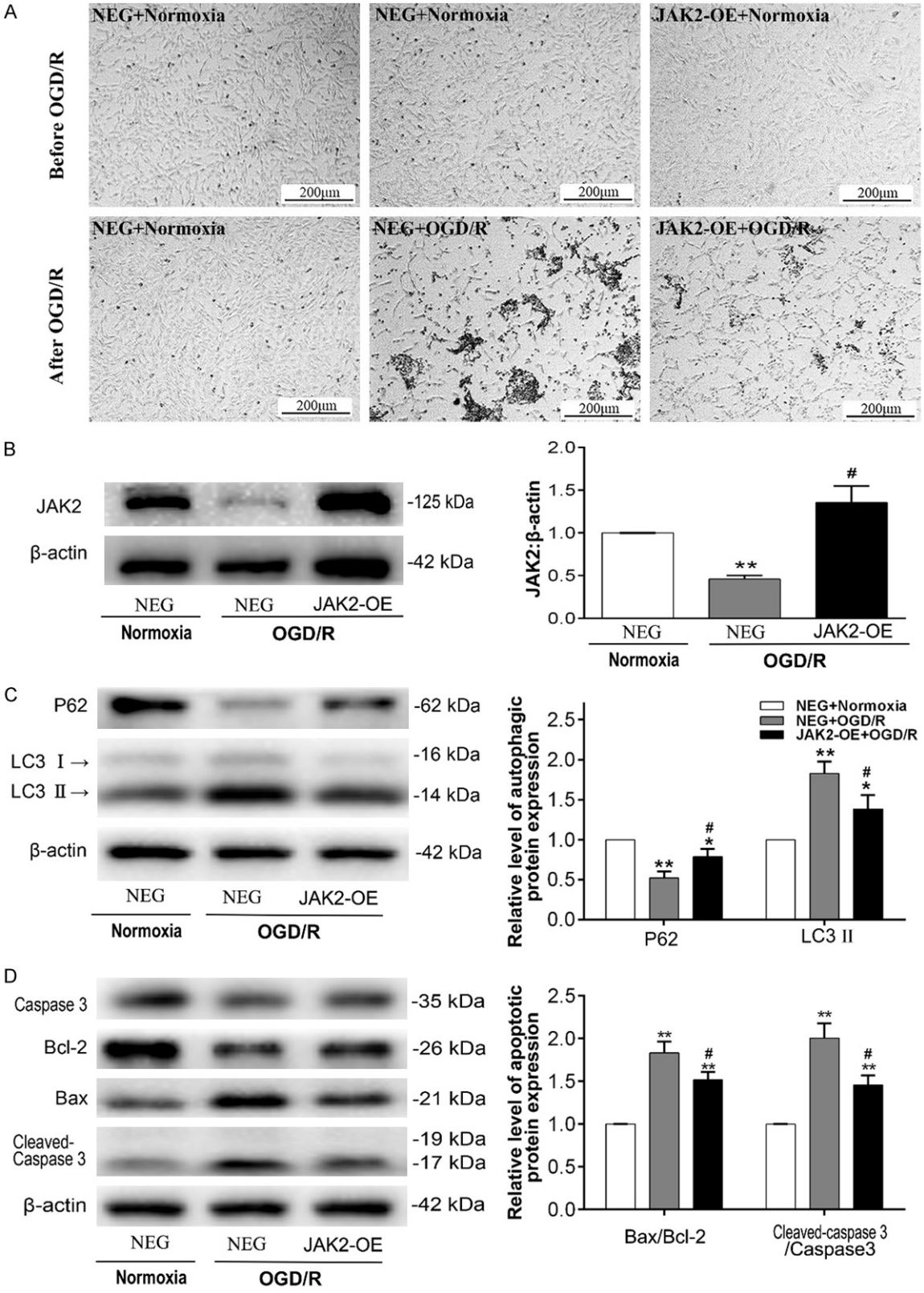

Figure 5. JAK2 overexpression inhibits OGD/R-induced autophagy and apoptosis in C2C12 myoblasts. C2C12 myoblast cells were transfected with lentivirus carrying JAK2 plasmid (JAK2-OE) or a negative control plasmid (NEG), exposed to normoxia (control group) or OGD/R. A. Light microscope photographs of C2C12 myoblast cells (JAK2-OE and/or NEG) exposed to normoxia (control group) or OGD/R, the scale was shown in corresponding picture. B.

Representative immunoblot images and relative quantification of JAK2; C. Representative immunoblot images and relative quantification of P62 and LC3, collectively an index of autophagy flux; D. Representative immunoblot images of Caspase 3, Bcl-2, Bax, cleaved Caspase 3 and relative quantification of Bax/Bcl-2 ratio and cleaved Caspase 3/Caspase 3 ratio, collectively an index of apoptosis level. Quantification expressed as fold induction over control group (assumed as 1), data were determined by densitometric analysis from at least 3 independent experiments after normalization by β-actin (Means ± SD; $*P < 0.05$, $**P < 0.01$ versus control group; $^{\#}P < 0.05$, $^{\#\#}P < 0.01$ versus NEG+OGD/R group).

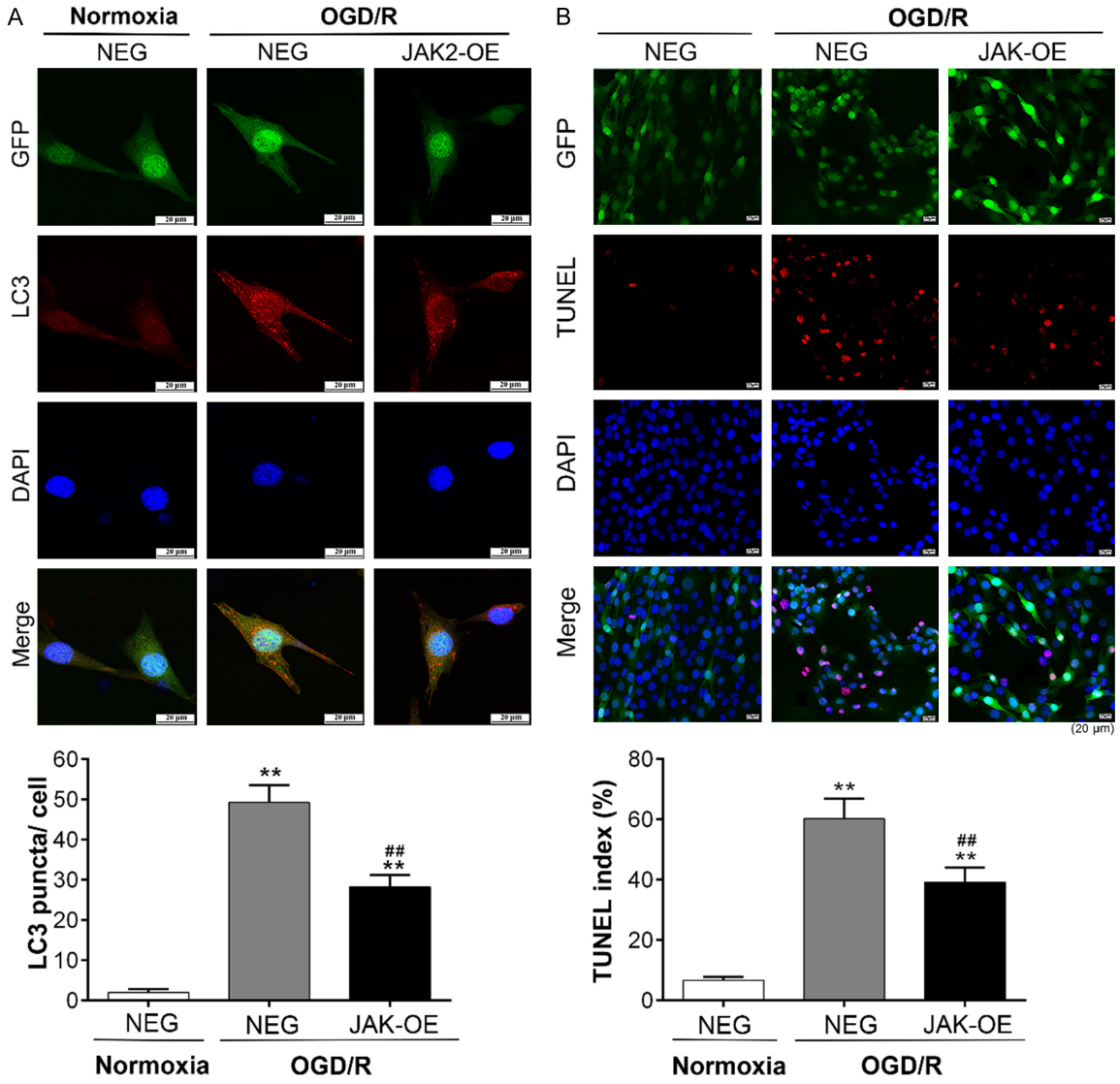

Figure 6. Immunofluorescence analysis of LC3 expression and TUNEL staining. The cells were transfected with EGFP-tagged lentivirus carrying JAK2 plasmid (JAK2-OE) or a negative control plasmid (NEG). A. Representative immunofluorescent photographs of LC3 expression in C2C12 myoblasts after normoxia (control group) or OGD/R treatment, and quantitative analysis was conducted to count the number of LC3-positive puncta per cell. B. Representative photomicrographs of TUNEL-stained C2C12 myoblast cells after normoxia (control group) or OGD/R treatment, and quantitative analysis of the number of apoptotic cells was shown as TUNEL index for different groups. The data were derived from three independent experiments (Means ± SD; $**P < 0.01$ versus control group; $^{\#\#}P < 0.01$ versus NEG+OGD/R group).

insult. In addition, C/EBP-Homologous Protein (CHOP), known to be an ERS marker, was significantly increased (**Figure 4**). As ERS is an important pathological mechanism of I/R injury, this result also implied that we have successfully built the I/R insult model in vitro.

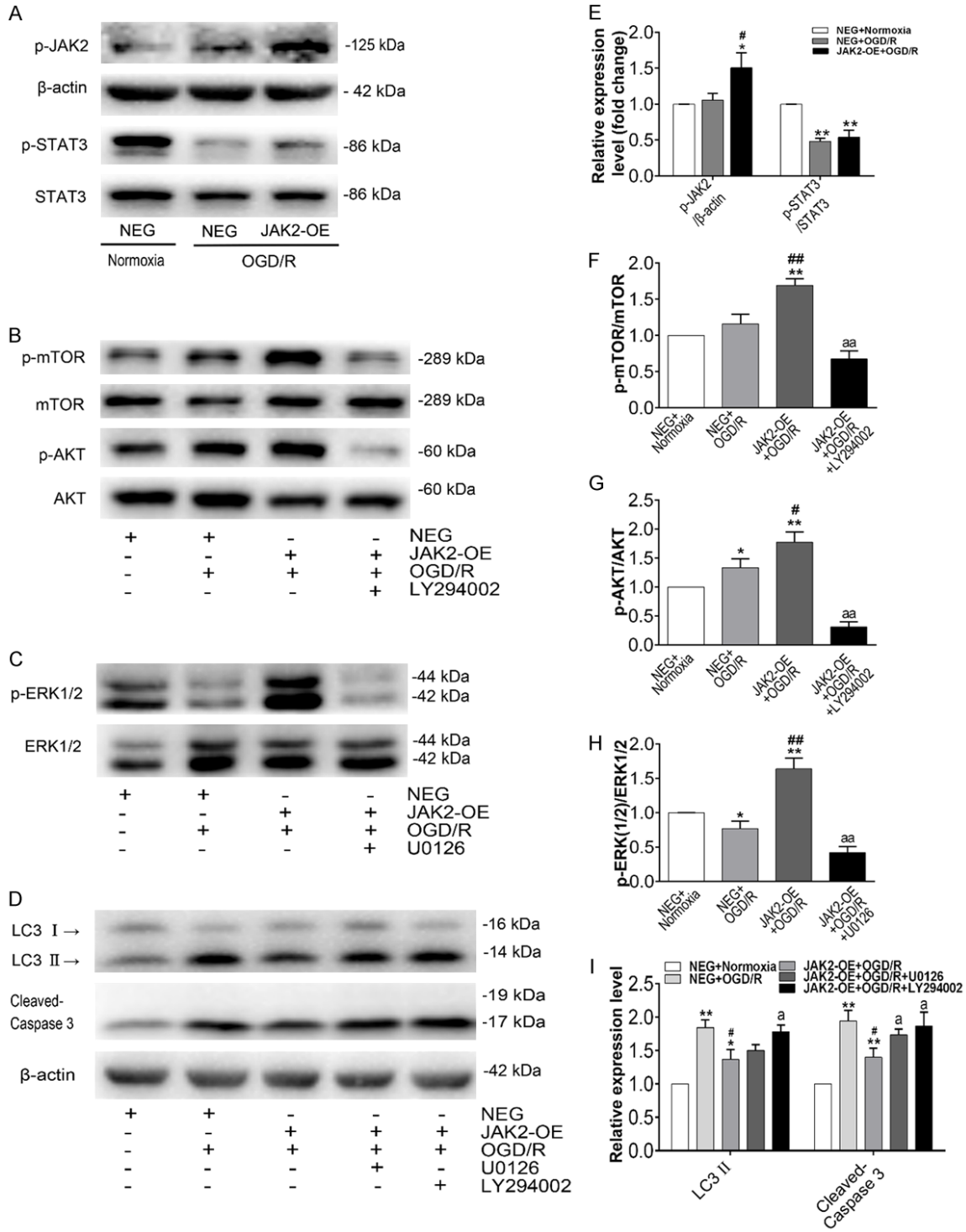

Figure 7. Representative protein expression of the JAK2/STAT3, AKT/mTOR, and ERK1/2 pathways. Western blot analysis of the total protein fraction from C2C12 myoblasts transfected with lentivirus carrying JAK2 plasmid (JAK2-OE) or a negative control plasmid (NEG), with normoxia (control group) or OGD/R treatment. The inhibitors LY294002 (10 μM) and U0126 (10 μM) were added to the medium 30 min before each experiment. (A) Representative immunoblot images of phosphorylated JAK2, total and phosphorylated STAT3; (B) Representative immunoblot images of total and phosphorylated mTOR, total and phosphorylated AKT; (C) Representative immunoblot images of total and phosphorylated ERK1/2; (D) Representative immunoblot images of LC3 and cleaved Caspase 3. Relative quantification of p-JAK2 and the ratios of p-STAT3/STAT3 (E), the ratio of p-mTOR/mTOR (F), the ratio of p-AKT/AKT (G), the ratio of p-ERK(1/2)/ERK(1/2) (H), and LC3 II and cleaved Caspase 3 (I), determined by densitometric analysis. Values were expressed as the means ± SD for three independent experiments. $^{*}P < 0.05$, $^{**}P < 0.01$ versus control group; $^{\#}P < 0.05$, $^{\#\#}P < 0.01$ versus NEG+OGD/R group; $^{a}P < 0.05$, $^{aa}P < 0.01$ versus JAK2-OE+OGD/R group.

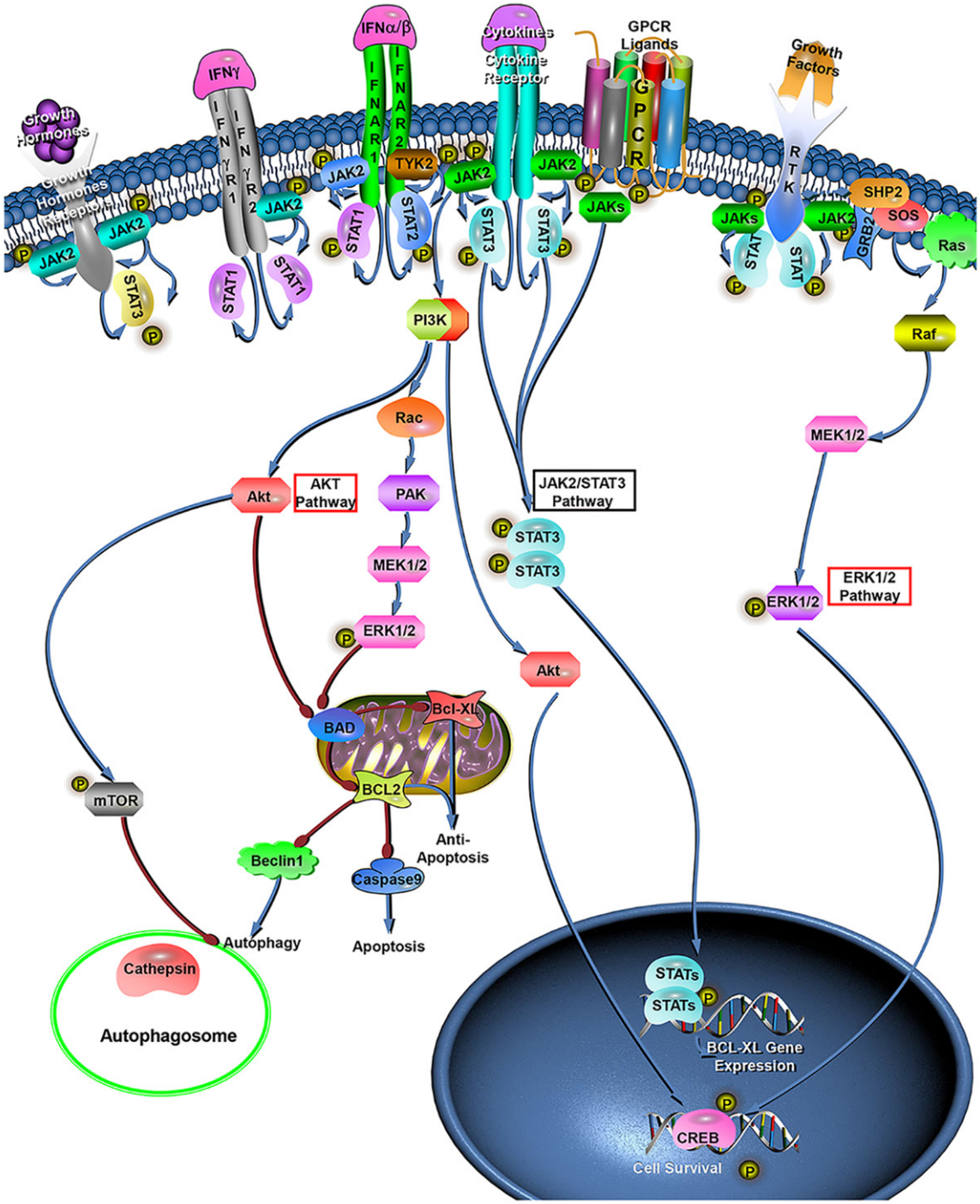

This image is a modification of QIAGEN's original, copyrighted image by Zan Liu. The original image may be found at www.qiagen.com/cn/shop/genes-and-pathways/pathway-details/?pwid=263

Figure 8. JAK2 overexpression alleviates C2C12 myoblasts I/R injury through the AKT and ERK1/2 pathway. As JAK2 is overexpressed in C2C12 myoblasts cells, the same extracellular stimuli will activate more JAK2, leading to its phosphorylation. Phosphorylated JAK2 can activate PI3K and Ras but without STAT3, resulting in activation of the AKT and ERK1/2 signaling pathway, which further activates mTOR and promotes Bcl-2, Bcl-XL and CREB up-regulation and caspase 9 down-regulation, contributing to inhibition of autophagy and apoptosis and thus making JAK2 perform an important protective role in I/R injury. (*Bad*: Bcl-xL/Bcl-2-associated death promoter; *CREB*: cAMP regulatory-binding protein; *Bcl-2*: B-cell lymphoma-2; *Bcl-XL*: B-cell lymphoma-extra large).

JAK2 overexpression inhibits OGD/R-induced autophagy and apoptosis and promotes myoprotection of C2C12 myoblasts exposed to OGD/R

Intriguingly, consistent with our previous series of experiments, significantly low expression of JAK2 was detected in the OGD/R experiment (**Figures 4** and **5B**). Reasoning that JAK2 may play a crucial role during I/R injury in muscle cells, we transfected C2C12 cells with lentivirus carrying EGFP-tagged JAK2 plasmid (JAK2-OE), which negated the down-regulation in JAK2 expression in the OGD/R experiment (**Figure 5B**, Supplementary Figure 2). The findings of light microscopy showed that the highest numbers of floating and aggregating C2C12 myoblasts, usually means cell death, were observed in the NEG group exposed to OGD/R, while cell death in JAK2-OE group was relatively less (**Figure 5A**). As shown in **Figure 5C** and **5D**, decreases in LC3II and the ratios of Bax/Bcl-2 and cleaved caspase 3/caspase 3 and an increase in p62 were evident in JAK2-OE group compared with the NEG group during OGD/R insult. LC3, once autophagy is activated, will localize into dot cytoplasmic structures (i.e., the autophagic vesicles). The confocal immunofluorescence analysis of LC3 expression indicated that relatively less accumulation of LC3 puncta was found in the JAK2-OE group than in the NEG group after OGD/R treatment, while a diffuse cytoplasmic distribution was observed in the normoxia treatment (**Figure 6A**). Additionally, in consonance with findings of light microscopy, the TUNEL assays confirmed that apoptotic myoblasts decreased in the JAK2-OE group compared with the NEG group after OGD/R treatment (**Figure 6B**). These results illustrated that JAK2 mediated the protective effect during muscular I/R injury by inhibition of autophagy and apoptosis in vitro.

AKT and ERK1/2, but irrespective of STAT3, pathways are involved in JAK2 overexpression-mediated autophagy and apoptosis inhibition

To dissect the JAK2 overexpression-associated signaling pathways involved in OGD/R-induced autophagy and apoptosis, the levels of expression and activation of some key proteins in the JAK2/STAT3, AKT and ERK1/2 pathways were analysed. The rationale for investigating AKT and ERK1/2 pathways is that JAK2 may provide upstream initiation of those two signaling pathways. As shown in **Figure 7A** and **7E**, immunoblot analysis indicated that p-JAK2 was significantly elevated in the JAK2-OE group compared with the NEG group. Surprisingly, the ratio of p-STAT3/STAT3 was reduced compared with the normal group and without significant difference between the NEG and JAK2-OE groups during OGD/R insult. Instead, the ratios of p-AKT/AKT and p-mTOR/mTOR were all elevated in the JAK2-OE group, suggesting activation of the AKT pathway (**Figure 7B**, **7F** and **7G**). In addition, strong activation of ERK1/2 was also found in the JAK2-OE group (**Figure 7C** and **7H**). These results showed an agreement with the pathway analysis based on proteomic data of PU muscle tissues. Furthermore, addition with PI3K/AKT inhibitor LY294002 and ERK 1/2 inhibitor U0126 during OGD/R experiment attenuated JAK2 mediated myoprotection, as indicated by a significant increase in cleaved caspase 3 and/or LC3II protein levels respectively (**Figure 7D** and **7I**). Thus, these results revealed that the myoprotective effects against I/R injury conferred by JAK2 may be mediated by the AKT and ERK1/2 pathway rather than STAT3 pathway.

Discussion

Deep PUs, necessarily involving DTI, usually arise in subcutaneous muscle layers adjacent to bony prominences owing to sustained unrelieved loading. Unfortunately, DTI is difficult to identify at an early stage and rapidly deteriorates to stage III or IV deep PUs, i.e., DTI can be a trigger of deep PUs. However, the molecular and cellular mechanisms accounting for the pathogenesis of DTI formation and deterioration remain unclear. Here, the present study showed that both autophagy and apoptosis were distinctly increased in deep PU muscle tissues. We then utilized LC-MS/MS analysis to systematically detect the protein expression profile in deep PU muscle tissues for the first time, which identified that JAK2 expression was distinctly decreased. Previous studies showed that deletion of JAK2 resulted in reduced quiescence and increased apoptosis in LSK cells, as well as impaired autophagy completion and podocyte function in mice [26, 27]. Moreover, it also plays a critical role in myocardial and cerebral I/R injury, but little is known about its role in skeletal muscle injury. In this study, JAK2

was overexpressed in C2C12 myoblasts followed by OGD/R insult for mimicking muscular I/R injury. The results illustrated that JAK2 overexpression efficiently inhibited OGD/R-induced autophagy and apoptosis and promoted myoprotection in myoblasts. Moreover, the AKT and ERK1/2 pathways were found to be involved in this process. It should be noted that the reason why JAK2 decreased in muscle tissue of deep PUs and C2C12 myoblasts exposed to OGD/R is not clear, and the mechanism warrants further research. In addition, we concentrated on elaborating the protective role of JAK2 just from its protein expression level. Thus, it is best to conduct additional experiments to explore more precise and meaningful roles of JAK2, in which activators may be applied. However, as far as we know, there is no specific JAK2 activator at present. Despite this, our study can clearly indicate that JAK2 plays an important protective role in deep PU development.

Autophagy and apoptosis are the necessary cellular processes orchestrated by intricate and interrelated networks. Although there are obvious differences between autophagy and apoptosis, many studies show that there is an ambiguous relationship between them. In most cases, it is well known that induction of autophagy can inhibit apoptosis and then protect the cells, and vice versa [28]. In contrast, autophagy is considered essential for the occurrence of apoptosis [29, 30]. In addition, some researchers suggest that autophagy and apoptosis can be converted to each other and exert synergetic effects [16, 31]. The results of this study, conforming to the report of Tam et al. [17], showed that autophagy and apoptosis were enormously elevated in deep PU muscle, implying they might play synergistic roles in the pathogenesis of DTI. However, by using an animal PU model, Teng et al. found that there were opposing responses of apoptosis and autophagy to moderate compression of skeletal muscle [32], and as they elaborated, inhibition of autophagy in the compressed muscles may be attributed to the elevation of Bcl-2, which can function as an anti-autophagic factor through disruption of the autophagic function of Beclin1.

Recent studies have illustrated that I/R injury has been regarded as the major contributing determinant in the occurrence of PUs [6]. On one hand, I/R injury can lead to an increase in intracellular autophagosomes/autophagy lysosomes [33], which can amplify apoptotic cascades, resulting in the promotion of apoptosis through regulating the “crosstalk” proteins (e.g., Beclin1, Bcl-2) interacting with apoptosis, and promote cell death, resulting in an aggravation of tissue damage by causing intracellular damage and bioenergetic dysfunction. On the other hand, I/R injury can cause oxidative stress, Ca^{2+} overload and an inflammatory response, resulting in ERS, which then induces the activation of the cell apoptosis pathway and causes irreversible tissue injury. In addition, a mounting number of studies have indicated that ERS is a potent inducer of autophagy in organisms from yeast to mammals [34]. Moreover, studies have shown that ERS-dependent autophagic cell death involved in muscle fibre damage in skeletal muscle diseases [35], which agrees with our result showing that autophagosomes and autophagic markers such as Beclin1, ATG5 and LC3II were significantly augmented in deep PU muscle.

Subsequently, we identified 520 differentially expressed proteins using proteomics, which permits simultaneous unbiased quantitative profiling of massive proteins from biological samples, aiming to explore key molecules and pathways associated with the development of deep PUs. Consequently, autophagy- and apoptosis-related proteins were highly enriched, some interacting with each other, and were implicated in a variety of pathways, such as the MAPK and PI3K/AKT signaling pathways. The present study showed that JAK2, which is ubiquitously expressed and plays an important role in cellular survival [26], was significantly downregulated in deep PU muscle. Given the poor understanding of its role in development of DTI in deep PUs, we further targeted JAK2 for in vitro I/R experimentation to test the hypothesis that JAK2 plays an important role during muscular I/R injury.

The OGD/R experiment is a generally accepted and adopted model to simulate I/R injury in vivo. Intriguingly, the expression of JAK2 was also decreased significantly following OGD/R insult in C2C12 myoblasts, accompanied by an elevation in autophagy and apoptosis. Previous studies also indicated that OGD/R injury could induce autophagy and apoptosis evidently [36, 37]. In the present study, we found that the expression of CHOP was significantly increased during OGD/R insult, and the aberrant increase

in CHOP has been proven to be associated with ERS, which contributes to apoptosis induction and autophagy activation in the process of I/R injury [38, 39]. However, the roles of autophagy in I/R injury are highly controversial. The crosstalk between autophagy and apoptosis may account for the dual roles of autophagy in various pathophysiological conditions. Autophagy may contribute to I/R damage via direct autophagic cell death or indirect switching of cell injury to apoptosis. The latter may result from increased cathepsins (e.g., Cathepsin B) accompanied by activation of autophagy, which plays a vital role in the caspase family activation and the subsequent apoptosis [39]. On the other hand, autophagy may function as a protective process during I/R injury, and inhibition of autophagy exacerbates injury induced by I/R.

In consonance with previous studies furnishing compelling evidence for an important protective role of JAK2, the present study verified that JAK2 promoted myoprotection against I/R injury, as evidenced by decreased apoptosis index and lower cell death ex vivo. In our experiments, JAK2 overexpression inhibited OGD/R-induced autophagy indicated by decreases in LC3II protein level and accumulation of LC3 puncta and an increase in p62. Note that current technologies to estimate autophagy flux are generally confined to multiple static measurements; autophagy activators and inhibitors (e.g., SAHA, 3-MA and Bafilomycin A1) should be additionally used to better distinguish autophagy flux, as well as further elaborate the relationship between autophagy and apoptosis during I/R injury. Previous studies have elucidated that activation of autophagy induces and aggravates cell death, while inhibition of autophagy can ameliorate cell death during I/R injury [11, 17, 36, 40], our data confirmed that the myo-protective role mediated by JAK2 was attributed to its suppression of autophagy and apoptosis in response to I/R injury. That said, depending on the environmental stressors, autophagy may play the distinct roles during different phases of I/R injury, and even the opposite [39, 41]. Our results support the overall hypothesis that both autophagy and apoptosis contribute to muscle damage resulting from I/R injury during the development of deep PUs, nevertheless, many more precise studies are required to further assess the roles of JAK2 in different phases of I/R injury.

Ultimately, as previous studies reported that JAK2/STAT3 is a powerful survival signalling pathway in many systems and that activation of this pathway protects cardiomyocytes against apoptosis in vitro and in vivo [42, 43], the molecular pathways involved in our OGD/R model were dissected (**Figure 8**). In the current study, since JAK2 was overexpressed, i.e., the substrate increased, the same extracellular and intracellular stimuli (e.g., cytokines, oxidative stress [44]) activated more JAK2. Surprisingly, the phosphorylated STAT3 remained basically unchanged while the phosphorylation level of JAK2 ascended, and instead, phosphorylated AKT, mTOR and ERK1/2 increased. Akada et al. found that activation of AKT and ERK1/2 was markedly reduced in JAK2-deficient LSK cells [26], conversely, our data showed that the AKT/mTOR and ERK1/2 pathways could be activated directly by phosphorylated JAK2. It is well known that activation of mTOR inhibits autophagy by suppression of autophagosome formation and autophagy initiation, and increases in Bcl-2 also restrain autophagy by binding to Beclin-1. Mounting studies have indicated that both AKT and ERK1/2 pathways participated in apoptosis inhibition and protection against myocardial and cerebral I/R injury [45, 46]. Actually, AKT and ERK1/2, considered survival factors, exert anti-apoptotic effects through phosphorylating a number of apoptosis regulatory molecules such as cAMP regulatory-binding protein (CREB) and Bcl-xL/Bcl-2-associated death promoter (BAD). The broad scope of AKT and ERK1/2 places them at the centre of multiple critical steps, giving them an important protective role to perform in various organs suffering I/R injury.

In summary, our results demonstrated that both autophagy and apoptosis are involved in muscle damage of deep PUs, and JAK2 may exerts protective effects against muscular I/R injury through suppression of autophagy and apoptosis. Thus, it is a reasonable speculate that JAK2 may be a potential therapeutic avenue for deep PUs. Of note, mechanism of down-regulation of JAK2 in deep PU muscle warrants further research.

Acknowledgements

This work was supported by grants from the National Natural Science Foundation of China (No. 81272091 & No. 81772084 to P.H.Z.), The Hunan Province Natural Science Foundation of

China (No. 2017JJ2396 to L.C.R.). Thanks are due to Professor Xue-Ping Feng for assistance with confocal photography and to professor Jun-Pu Wang for valuable guidance of reading electron microscope images.

Disclosure of conflict of interest

None.

Address correspondence to: Pihong Zhang, Department of Burns and Reconstructive Surgery, Xiangya Hospital, Central South University, 87 Xiangya Road, Changsha 410008, Hunan, P. R. China. Tel: +86 731 89753713; E-mail: zphong@aliyun.com

References

[1] Stekelenburg A, Gawlitta D, Bader DL and Oomens CW. Deep tissue injury: how deep is our understanding? Arch Phys Med Rehabil 2008; 89: 1410-1413.

[2] Hoogendoorn I, Reenalda J, Koopman B and Rietman JS. The effect of pressure and shear on tissue viability of human skin in relation to the development of pressure ulcers: a systematic review. J Tissue Viability 2017; 26: 157-171.

[3] Smith ME, Totten A, Hickam DH, Fu R, Wasson N, Rahman B, Motu'apuaka M and Saha S. Pressure ulcer treatment strategies: a systematic comparative effectiveness review. Ann Intern Med 2013; 159: 39-50.

[4] Bass MJ and Phillips LG. Pressure sores. Curr Probl Surg 2007; 44: 101-143.

[5] Berlowitz DR and Brienza DM. Are all pressure ulcers the result of deep tissue injury? A review of the literature. Ostomy Wound Manage 2007; 53: 34-38.

[6] Cui FF, Pan YY, Xie HH, Wang XH, Shi HX, Xiao J, Zhang HY, Chang HT and Jiang LP. Pressure combined with ischemia/reperfusion injury induces deep tissue injury via endoplasmic reticulum stress in a rat pressure ulcer model. Int J Mol Sci 2016; 17: 284.

[7] Lockshin RA and Zakeri Z. Apoptosis, autophagy, and more. Int J Biochem Cell Biol 2004; 36: 2405-2419.

[8] Neel BA, Lin Y and Pessin JE. Skeletal muscle autophagy: a new metabolic regulator. Trends Endocrinol Metab 2013; 24: 635-643.

[9] Masiero E, Agatea L, Mammucari C, Blaauw B, Loro E, Komatsu M, Metzger D, Reggiani C, Schiaffino S and Sandri M. Autophagy is required to maintain muscle mass. Cell Metab 2009; 10: 507-515.

[10] Masiero E and Sandri M. Autophagy inhibition induces atrophy and myopathy in adult skeletal muscles. Autophagy 2010; 6: 307-309.

[11] Sun D, Wang W, Wang X, Wang Y, Xu X, Ping F, Du Y, Jiang W and Cui D. bFGF plays a neuroprotective role by suppressing excessive autophagy and apoptosis after transient global cerebral ischemia in rats. Cell Death Dis 2018; 9: 172.

[12] Adhihetty PJ, O'Leary MF, Chabi B, Wicks KL and Hood DA. Effect of denervation on mitochondrially mediated apoptosis in skeletal muscle. J Appl Physiol (1985) 2007; 102: 1143-1151.

[13] Lee G, Lim JY and Frontera WR. Apoptosis in young and old denervated rat skeletal muscle. Muscle Nerve 2017; 55: 262-269.

[14] Wang WZ, Fang XH, Stephenson LL, Khiabani KT and Zamboni WA. Ischemia/reperfusion-induced necrosis and apoptosis in the cells isolated from rat skeletal muscle. J Orthop Res 2008; 26: 351-356.

[15] Nakazawa H, Chang K, Shinozaki S, Yasukawa T, Ishimaru K, Yasuhara S, Yu YM, Martyn JA, Tompkins RG, Shimokado K and Kaneki M. iNOS as a driver of inflammation and apoptosis in mouse skeletal muscle after burn injury: possible involvement of sirt1 s-nitrosylation-mediated acetylation of p65 NF-kappaB and p53. PLoS One 2017; 12: e0170391.

[16] Maiuri MC, Zalckvar E, Kimchi A and Kroemer G. Self-eating and self-killing: crosstalk between autophagy and apoptosis. Nat Rev Mol Cell Biol 2007; 8: 741-752.

[17] Tam BT, Yu AP, Tam EW, Monks DA, Wang XP, Pei XM, Koh SP, Sin TK, Law HKW, Ugwu FN, Supriya R, Yung BY, Yip SP, Wong SC, Chan LW, Lai CW, Ouyang P and Siu PM. Ablation of Bax and Bak protects skeletal muscle against pressure-induced injury. Sci Rep 2018; 8: 3689.

[18] O'Shea JJ, Holland SM and Staudt LM. JAKs and STATs in immunity, immunodeficiency, and cancer. N Engl J Med 2013; 368: 161-170.

[19] Mascareno E, El-Shafei M, Maulik N, Sato M, Guo Y, Das DK and Siddiqui MA. JAK/STAT signaling is associated with cardiac dysfunction during ischemia and reperfusion. Circulation 2001; 104: 325-329.

[20] Liu X, Zhang X, Zhang J, Kang N, Zhang N, Wang H, Xue J, Yu J, Yang Y, Cui H, Cui L, Wang L and Wang X. Diosmin protects against cerebral ischemia/reperfusion injury through activating JAK2/STAT3 signal pathway in mice. Neuroscience 2014; 268: 318-327.

[21] Yang N, Luo M, Li R, Huang Y, Zhang R, Wu Q, Wang F, Li Y and Yu X. Blockage of JAK/STAT signalling attenuates renal ischaemia-reperfusion injury in rat. Nephrol Dial Transplant 2008; 23: 91-100.

[22] Huang P, Zhou Y, Liu Z and Zhang P. Interaction between ANXA1 and GATA-3 in immunosuppression of CD4(+) T cells. Mediators Inflamm 2016; 2016: 1701059.

[23] Hsu PY, Hsi E, Wang TM, Lin RT, Liao YC and Juo SH. MicroRNA let-7g possesses a therapeutic potential for peripheral artery disease. J Cell Mol Med 2017; 21: 519-529.

[24] Han JH, Zhou W, Li W, Tuan PQ, Khoi NM, Thuong PT, Na M and Myung CS. Pentacyclic triterpenoids from Astilbe rivularis that enhance glucose uptake via the activation of Akt and Erk1/2 in C2C12 Myotubes. J Nat Prod 2015; 78: 1005-1014.
[25] Hwang SY, Kang YJ, Sung B, Kim M, Kim DH, Lee Y, Yoo MA, Kim CM, Chung HY and Kim ND. Folic acid promotes the myogenic differentiation of C2C12 murine myoblasts through the Akt signaling pathway. Int J Mol Med 2015; 36: 1073-1080.
[26] Akada H, Akada S, Hutchison RE, Sakamoto K, Wagner KU and Mohi G. Critical role of Jak2 in the maintenance and function of adult hematopoietic stem cells. Stem Cells 2014; 32: 1878-1889.
[27] Alghamdi TA, Majumder S, Thieme K, Batchu SN, White KE, Liu Y, Brijmohan AS, Bowskill BB, Advani SL, Woo M and Advani A. Janus kinase 2 regulates transcription factor eb expression and autophagy completion in glomerular podocytes. J Am Soc Nephrol 2017; 28: 2641-2653.
[28] Li X, Zhu F, Jiang J, Sun C, Zhong Q, Shen M, Wang X, Tian R, Shi C, Xu M, Peng F, Guo X, Hu J, Ye D, Wang M and Qin R. Simultaneous inhibition of the ubiquitin-proteasome system and autophagy enhances apoptosis induced by ER stress aggravators in human pancreatic cancer cells. Autophagy 2016; 12: 1521-1537.
[29] Lee TG, Jeong EH, Kim SY, Kim HR and Kim CH. The combination of irreversible EGFR TKIs and SAHA induces apoptosis and autophagy-mediated cell death to overcome acquired resistance in EGFR T790M-mutated lung cancer. Int J Cancer 2015; 136: 2717-2729.
[30] Saiki S, Sasazawa Y, Imamichi Y, Kawajiri S, Fujimaki T, Tanida I, Kobayashi H, Sato F, Sato S, Ishikawa K, Imoto M and Hattori N. Caffeine induces apoptosis by enhancement of autophagy via PI3K/Akt/mTOR/p70S6K inhibition. Autophagy 2011; 7: 176-187.
[31] Ouyang L, Shi Z, Zhao S, Wang FT, Zhou TT, Liu B and Bao JK. Programmed cell death pathways in cancer: a review of apoptosis, autophagy and programmed necrosis. Cell Prolif 2012; 45: 487-498.
[32] Teng BT, Pei XM, Tam EW, Benzie IF and Siu PM. Opposing responses of apoptosis and autophagy to moderate compression in skeletal muscle. Acta Physiol (Oxf) 2011; 201: 239-254.
[33] Suzuki C, Isaka Y, Takabatake Y, Tanaka H, Koike M, Shibata M, Uchiyama Y, Takahara S and Imai E. Participation of autophagy in renal ischemia/reperfusion injury. Biochem Biophys Res Commun 2008; 368: 100-106.
[34] Hoyer-Hansen M and Jaattela M. Connecting endoplasmic reticulum stress to autophagy by unfolded protein response and calcium. Cell Death Differ 2007; 14: 1576-1582.
[35] Madaro L, Marrocco V, Carnio S, Sandri M and Bouche M. Intracellular signaling in ER stress-induced autophagy in skeletal muscle cells. FASEB J 2013; 27: 1990-2000.
[36] Fan J, Liu Y, Yin J, Li Q, Li Y, Gu J, Cai W and Yin G. Oxygen-glucose-deprivation/reoxygenation-induced autophagic cell death depends on JNK-mediated phosphorylation of Bcl-2. Cell Physiol Biochem 2016; 38: 1063-1074.
[37] Shang X, Bao Y, Chen S, Ren H, Huang H and Li Y. Expression and purification of TAT-fused carbonic anhydrase III and its effect on C2C12 cell apoptosis induced by hypoxia/reoxygenation. Arch Med Sci 2012; 8: 711-718.
[38] Senft D and Ronai ZA. UPR, autophagy, and mitochondria crosstalk underlies the ER stress response. Trends Biochem Sci 2015; 40: 141-148.
[39] Sheng R and Qin ZH. The divergent roles of autophagy in ischemia and preconditioning. Acta Pharmacol Sin 2015; 36: 411-420.
[40] Mo ZT, Fang YQ, He YP and Zhang S. Beta-Asarone protects PC12 cells against OGD/R-induced injury via attenuating Beclin-1-dependent autophagy. Acta Pharmacol Sin 2012; 33: 737-742.
[41] Chen G, Zhang W, Li YP, Ren JG, Xu N, Liu H, Wang FQ, Sun ZJ, Jia J and Zhao YF. Hypoxia-induced autophagy in endothelial cells: a double-edged sword in the progression of infantile haemangioma? Cardiovasc Res 2013; 98: 437-448.
[42] Jiang X, Guo CX, Zeng XJ, Li HH, Chen BX and Du FH. A soluble receptor for advanced glycation end-products inhibits myocardial apoptosis induced by ischemia/reperfusion via the JAK2/STAT3 pathway. Apoptosis 2015; 20: 1033-1047.
[43] La Fortezza M, Schenk M, Cosolo A, Kolybaba A, Grass I and Classen AK. JAK/STAT signalling mediates cell survival in response to tissue stress. Development 2016; 143: 2907-2919.
[44] Sandberg EM and Sayeski PP. Jak2 tyrosine kinase mediates oxidative stress-induced apoptosis in vascular smooth muscle cells. J Biol Chem 2004; 279: 34547-34552.
[45] Yin Y, Guan Y, Duan J, Wei G, Zhu Y, Quan W, Guo C, Zhou D, Wang Y, Xi M and Wen A. Cardioprotective effect of Danshensu against myocardial ischemia/reperfusion injury and inhibits apoptosis of H9c2 cardiomyocytes via Akt and ERK1/2 phosphorylation. Eur J Pharmacol 2013; 699: 219-226.
[46] Zhu YM, Wang CC, Chen L, Qian LB, Ma LL, Yu J, Zhu MH, Wen CY, Yu LN and Yan M. Both PI3K/Akt and ERK1/2 pathways participate in the protection by dexmedetomidine against transient focal cerebral ischemia/reperfusion injury in rats. Brain Res 2013; 1494: 1-8.

Supplementary Table 1. Clinical characteristics of patients with deep PU

Gender	Age	BMI# (Kg/m^2)	Etiology/Past Disease	Multi-morbidity	Ulceration Duration	Ulceration Position	Ulceration Size (cm^2)	Wound Infection	Hemoglo-bin (g/L)
M	18	19.3	Paraplegia	No	5 m	Sacrococcygeal	10 × 18	Yes	83
M	29	20.8	Traumatic Brain Injury	No	3 m	Sacrococcygeal	6 × 8	Yes	93
M	68	27.5	Postoperative Wound Infection	Yes	1 m	Sacrococcygeal	12 × 10	Yes	109
F	19	21.3	Multiple Trauma	Yes	1 m	Sacrococcygeal	6 × 7	Yes	97
F	29	23.7	Syringomyelia	No	12 m	Ischial tuberosity	5 × 5	Yes	90
M	74	27.5	Paraplegia	No	3 m	Sacrococcygeal	11 × 10	Yes	98
M	43	23.3	Paraplegia	No	6 m	Ischial tuberosity	11 × 10	Yes	134
M	26	39.2	Severe Acute Pancreatitis	Yes	3 m	Sacrococcygeal	7 × 8	Yes	97
F	39	22.1	Paraplegia	No	3 m	Sacrococcygeal	8 × 8	Yes	101
M	40	25.6	Paraplegia	No	8 m	Greater trochanter	10 × 8	Yes	145
M	32	22.3	Paraplegia	Yes	10 m	Ischial tuberosity	6 × 5	Yes	68

#: Body Mass Index.

Supplementary Table 2. Primary antibodies used in this study

Cat. No.	Antibody	Source	Manufacturer	Town & State	Country	Dilution
3230	JAK2	Rabbit	CST	Beverly, MA	USA	1:1000
4406	p-JAK2 (Tyr1007)	Rabbit	CST	Beverly, MA	USA	1:1000
4904	STAT3	Rabbit	CST	Beverly, MA	USA	1:2000
9145	p-STAT3 (Tyr705)	Rabbit	CST	Beverly, MA	USA	1:2000
4691	AKT (pan)	Rabbit	CST	Beverly, MA	USA	1:1000
4060	p-AKT (Ser473)	Rabbit	CST	Beverly, MA	USA	1:2000
4695	ERK1/2	Rabbit	CST	Beverly, MA	USA	1:1000
4370	p-ERK1/2(Thr202/Tyr204)	Rabbit	CST	Beverly, MA	USA	1:2000
2983	mTOR	Rabbit	CST	Beverly, MA	USA	1:1000
5536	p-mTOR (Ser2448)	Rabbit	CST	Beverly, MA	USA	1:1000
2895	CHOP	Mouse	CST	Beverly, MA	USA	1:1000
9662	Caspase-3	Rabbit	CST	Beverly, MA	USA	1:1000
2870	Bcl-2	Rabbit	CST	Beverly, MA	USA	1:1000
50599-2-Ig	Bax	Rabbit	ProteinTech	Chicago, IL	USA	1:2000
9661	Cleaved Caspase-3	Rabbit	CST	Beverly, MA	USA	1:1000
3495	Beclin-1	Rabbit	CST	Beverly, MA	USA	1:1000
5114	SQSTM1/P62	Rabbit	CST	Beverly, MA	USA	1:1000
12994	ATG5	Rabbit	CST	Beverly, MA	USA	1:1000
2775	LC3B	Rabbit	CST	Beverly, MA	USA	1:1000
4970	β-Actin	Rabbit	CST	Beverly, MA	USA	1:1000

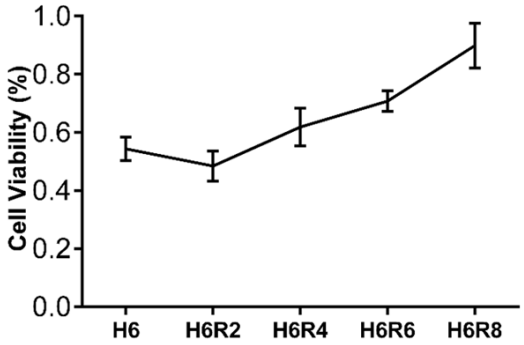

Supplementary Figure 1. Cell viability assay of C2C12 myoblasts exposed to OGD with different time periods of reoxygenation.

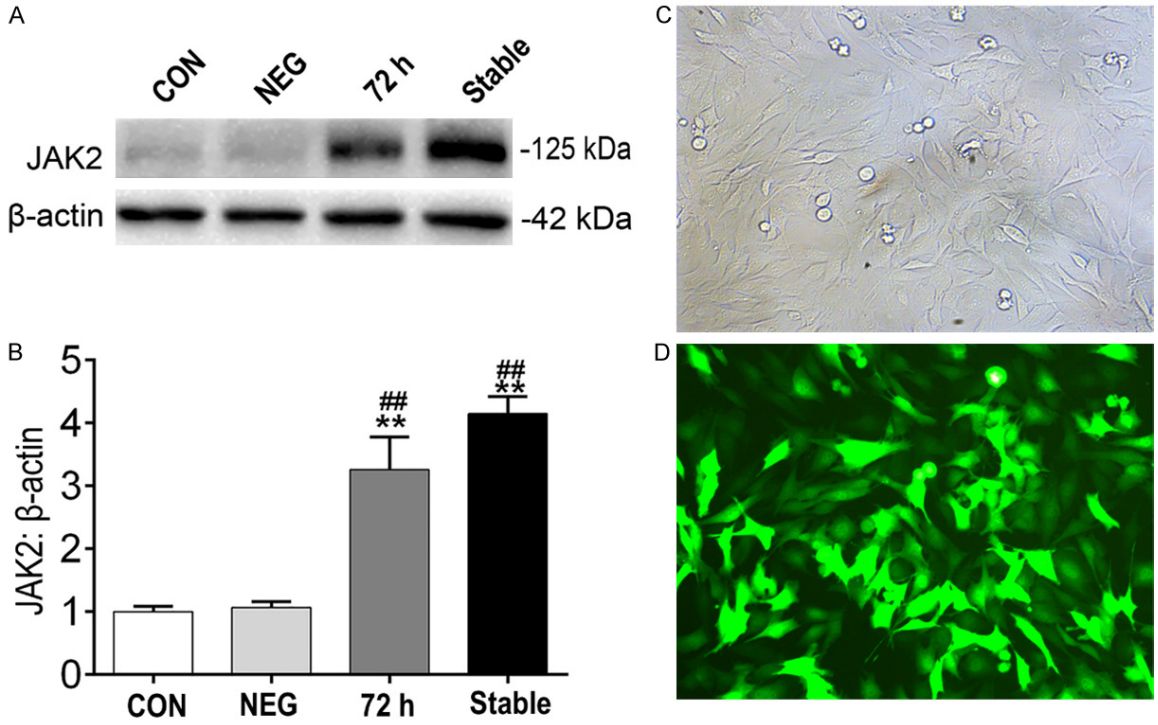

Supplementary Figure 2. Validation of JAK2 overexpression in C2C12 myoblast cells. A. Immunoblot images of JAK2 and β-actin in C2C12 myoblasts, which were transfected with lentivirus carrying a negative control (NEG) plasmid and JAK2 plasmid after 72 h (72 h) or selection with puromycin (Stable). B. Relative quantification of JAK2 after normalization by β-actin, the data were derived from three independent experiments (Means ± SD; $^{**}P < 0.01$ versus Control; $^{\#\#}P < 0.01$ versus NEG). C. Light microscope photographs of C2C12 myoblast cells. D. Fluorescent photographs of EGFP expression in JAK2-overexpressed C2C12 myoblast cells.